International Journal of Computing and Digital Systems
ISSN (2210-142X)
Int. J. Com. Dig. Sys.13, No.1 (May-23)

http://dx.doi.org/10.12785/ijcds/1301120

Current Reduction in Electrical Vehicles via EPAS System Control using MVO and GWO based Tuning Methodology

Vinod Kumar[1], Gunjan Chorasiya[1] and Sathans Suhag[2]

[1]*Department of Electrical Engineering, Indian Institute of Technology, Delhi, India*
[2]*Department of Electrical Engineering, National Institute of Technology, Kurukshetra, Haryana, India*

Received 10 Apr. 2022, Revised 30 Apr. 2023, Accepted 14 May. 2023, Published 30 May. 2023

Abstract: The electric power assist steering (EPAS) system has, in the recent years, emerged as an effective alternative to the conventional hydraulic powered steering system in new vehicles owing to its significant potential in minimizing energy utilization and enhancing the efficiency of driving performance. In all new electrical vehicular technology, for all sub-systems, there is a requirement of battery energy; hence energy conservation is the first essential criterion to be met. In this work, therefore, recent meta-heuristic techniques are implemented to optimally tune the proportional, integral, and derivative with filter (PIDF) controller, applied over the EPAS system, to realize the assist current reduction for its operation. The results establish the effectiveness of the novel proposition in reducing the assist current and minimizing the energy demand as compared to the conventional tuning. Apart from this, the drive torque is also reduced. Matlab® platform is used for modelling and simulations.

Keywords: Electric power assist steering system (EPAS); Multi-verse optimizer (MVO); Gray wolf optimization (GWO); Electric vehicle (EV); PIDF controller

1. Introduction

The generated pollution from the transport system is among the significant challenges to the environment and climate change in the world [1]. The adoption of electric vehicles (EVs) can be a practical and viable solution to deal with the pollution issue, and it will also improve transport system energy efficiency [2]. However, in EVs, the battery provides the only energy supply for its subsystems so, the capacity of the battery has been a prime concern in EV technology for long-range operations. Therefore, the challenge lies in minimizing the energy demand from the battery be it by the main driving motor or the subsystems. Because of this reason, both the earlier mechanical and hydraulic power-assisted steering systems are now outdated. The constant energy requirement from the battery for maintaining the hydraulic pump pressure and the regular maintenance in mechanical, hydraulic assisted power steering system contributed towards the replacement of traditional steering systems.

The EPAS system is one of the subsystems through which we can improve the EV's efficiency as it requires energy only in the event of the steering wheel being operated by the driver [3], unlike hydraulic power-assisted steering. The subsystem control flexibility gets increased because of the system being electronically coupled with the motor and as a result not complex in terms of configuration and is less-rigid. Its independence on engine, fuel economy, modularity, compact size, steering feel credibility, ease of assembly, and no adverse effects on the environment are some foremost advantages over the conventional system [4]. The EPAS system is depicted in Figure 1. Through an electric motor, EPAS generates required assist torque when a driver steers, which is sensed through torque sensor present between the steering wheel and mounted motor. The sensor provides an input signal to electric motor, which in turn sets up assist torque which helps reduced the torque actually applied through the driving wheel since generated assist torque is subsequently multiplied by the gear assembly, which in combination with the drive torque contributes towards the total steering torque. Feeling over the steering of the driver also improves because of this. The controller, which is usually PID and situated in the electronic control unit (ECU), is utilized to control the motor-assist current. To obtain optimal performance, the controller parameters: K_p, K_i, and K_d, have to be tuned such that the parameter setting used after tuning leads to less amount of current utilization. Several analyses on performance, design, and control have been conducted over the EPAS system. In [5], an optimal control strategy is derived. A similar analysis for sensor-less optimal control of the EPAS system is also reported in [6].

E-mail address: vinod.kumar@ee.iitd.ac.in, gunjan.chorasiya@ee.iitd.ac.in, sathans@nitkkr.ac.in

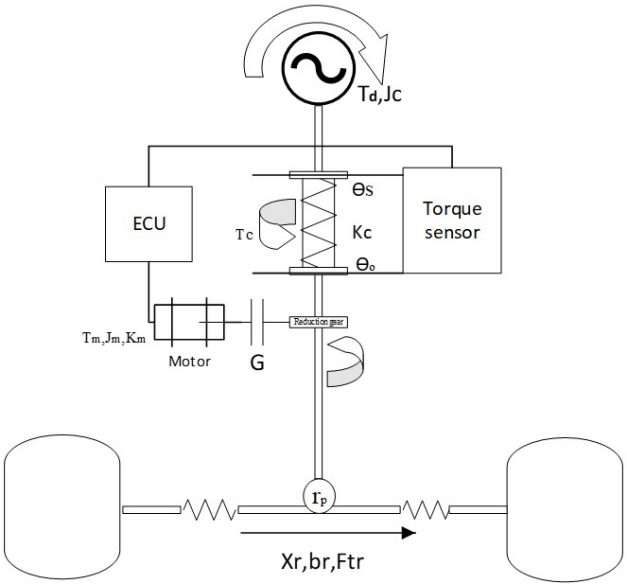

Figure 1. EPAS Schematic

For the disturbance rejection in the EPAS system optimally, control design is carried out in [7]. In another paper, linear quadratic gaussian (LQG) based optimal control design for EPAS is implemented [8]. Various other controller design approaches are applied over the system in [9], [10], [11], such as the Takagi-Sugeno fuzzy approach, linear quadratic regulator (LQR) approach, and sliding mode control. For the best performance within the parametric design under the influence of changes in the speed of vehicle and the road condition disturbance occurring externally, the work is reported in [12].

PID controller is fed with an adequate amount of current generated using booster curve or characteristic curve in [13], [14]. Chabaan and Wang used H_∞ control technique for generating assist torque in [15]. In [16], a novel control strategy is put forth using a reference model for getting desired performance in terms of drive torque, and steering wheel angle using the sliding mode controller. In [17], using analytical equations for EPAS system, genetic algorithm (GA) optimized EPAS control is presented. Similarly, particle swarm optimization (PSO) and ant colony optimization (ACO) tuned PID controller based current reduction is addressed in [18]. Also, power reduction and energy optimization are depicted in [19], [20]. A similar approach is used in [21] where the controller's role is to track the assisted current generated by the lookup table yet again. Here, the authors used fractional-Order PID (FOPID) controller and the Particle Swarm Optimization (PSO) method as tuning mechanism.

The traditional PID control method will result in poor dynamic performance or system instability when addressing the nonlinear frictional resistance problem of the electric power steering system. In [22], the proposed research offers a control technique based on PID parameter self-tuning using back propagation neural networks. Also, to discretize the vehicle's power assistance characteristic, authors in [22] proposed back propagation neural network arbitrary nonlinear approximations. The steering power is also realized across the entire speed range, overcoming the steering blind zone and laying the foundations for future controller design. For the steering wheel device to offer high maneuverability and the short learning period, a steer by wire steering is utilized in [23]. This is validated by changing parameters in accordance with system identification and measurements taken on the test rig. The proposed work was also tested on a Volvo S60 vehicle and the steering device was put to the test in real-world driving conditions. The proposed method performed well throughout testing, with surprisingly good drive-ability, after some vehicle adjustment.

In this paper, the potential and efficacy of grey wolf optimizer (GWO) and Multi-verse optimizer (MVO) as tuning methodologies for PIDF controller, as applied for EPAS system of Figure 1, is investigated and realized for Assist current reduction. The parameters of the EPAS system, given in Table I, are adapted from [16], and the equations describing the dynamic model are referred from [18].

2. System Modelling

The C (column) type EPAS configuration, depicted in Figure 1, is modeled and analyzed in terms of the mathematical description of the different sub-systems of its configuration which are

1) Steering column system design.
2) Assist motor and Sensor system design.
3) Rack and pinion system design.

The steering column sub-system equations, using Newton's Law of motion, are as follows:

$$J_c\ddot{\theta}_s + B_c\dot{\theta}_s + K_c(\theta_s - \theta_o) = T_d, \tag{1}$$

$$J_c\ddot{\theta}_s + B_c\dot{\theta}_s + K_c(\theta_s - \theta_o) = T_d + K_c\Big(\frac{X_r}{r_p}\Big). \tag{2}$$

Where, $\theta_o = \frac{X_r}{r_p}$

$$T_c = K_c(\theta_s - \theta_o). \tag{3}$$

Equations of motion for Assist motor section and its dynamics are given below:

$$J_m\ddot{\theta}_m + B_m\dot{\theta}_m + K_m(\theta_m - G\theta_o) = T_m, \tag{4}$$

$$T_m = K_e i_a, \tag{5}$$

$$T_a = K_m(\theta_m - G\theta_o), \tag{6}$$

$$J_m\ddot{\theta}_m + B_m\dot{\theta}_m + T_a = T_m, \tag{7}$$

$$V_a = Ri_a + L\frac{di}{dt} + K_a\dot{\theta}_m. \tag{8}$$

Equation (9) describes the force applied over the output axle of steering shaft whereas the equations (11) and (12)

TABLE I. EPAS SYSTEM PARAMETERS

Parameter	Value	Units
Moment of inertia of steering column (J_c)	0.04	Kgm^2
Viscous damping of Steering column (B_c)	0.072	$Nmsrad^{-1}$
Steering column stiffness(K_c)	115	$Nmsrad^{-1}$
Moment of inertia of motor (J_m)	0.0004	Kgm^2
Viscous damping of Motor (B_m)	0.0032	$Nmsrad^{-1}$
Stiffness of motor (K_s)	625	$Nmsrad^{-1}$
Rack Mass (M_r)	32	Kg
Viscous damping of Rack (b_r)	3820	$Nmsrad^{-1}$
Tire spring Rate (K_r)	43000	Nmm^{-1}
Inductance of motor (L)	0.0056	Henry
Motor Resistance (R)	0.37	$\Omega(ohm)$
Coefficient of motor torque (K_m)	0.05	NmA^{-1}
Coefficient of motor EMF (K_a)	0.05	$VS\,rad^{-1}$
Motor gear ratio G	13.65	-
Pinion Radius (r_p)	0.0071	m

express the rack and pinion section design and Tire friction force, respectively.

$$J_o\ddot{\theta}_o + B_o\dot{\theta}_o + T_l = K_c(\theta_s - \theta_o) + GT_a, \quad (9)$$

$$J_o\ddot{\theta}_o + B_o\dot{\theta}_o + T_l = K_c(\theta_s - \theta_o) + G[K_m(\theta_m - G\theta_o)], \quad (10)$$

$$T_l = T_a + T_c, \quad (11)$$

$$m_r\ddot{x} + b_r\dot{x} + K_r x = \frac{T_l}{r_p} - F_t, \quad (12)$$

$$F_t = K_r x + F_d. \quad (13)$$

Recombining and using substitutions, the three main equations for simulation modeling are as given below:

$$J_c\ddot{\theta}_s + B_c\dot{\theta}_s + K_c\theta_s = T_d + K_c(\frac{X_r}{r_p}), \quad (14)$$

$$J_m\ddot{\theta}_m + B_m\dot{\theta}_m = T_m + GK_s(\frac{X_r}{r_p}) - K_m\theta_m, \quad (15)$$

$$M\ddot{x} + B\dot{x} + Kx = \frac{K_c\theta_s}{r_p} + \frac{GK_s\theta_m}{r_p} - F_d, \quad (16)$$

(17)

Where,
$M = m_r + \frac{J_o}{r_p^2}$,
$B = b_r + \frac{B_o}{r_p^2}$,
$K = K_r + \frac{K_c}{r_p^2} + \frac{G^2K_s}{r_p^2}$.

The terms T_d, X_r, θ_m, T_a, T_l, θ_s, θ_o used here are drive torque, rack position, the angular displacement of the motor shaft, assist torque, load torque, input axle angular displacement, and output axle angular displacement respectively.

Figure 2 depicts the simulation model of the complete EPAS system, whereas Figure 3 shows the characteristics curve.

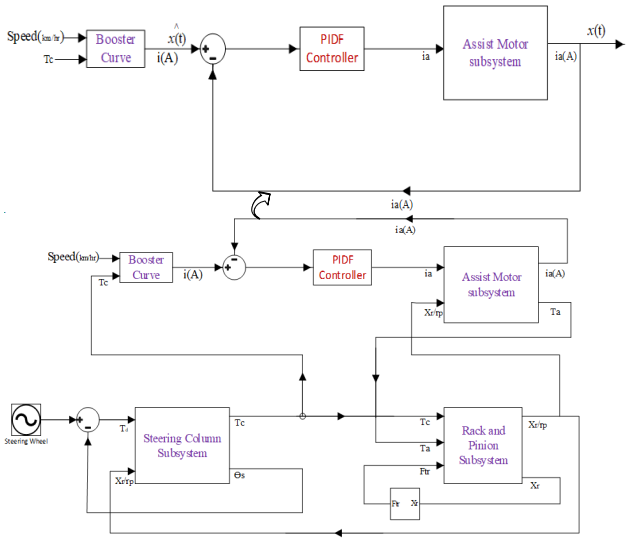

Figure 2. EPAS system simulation model

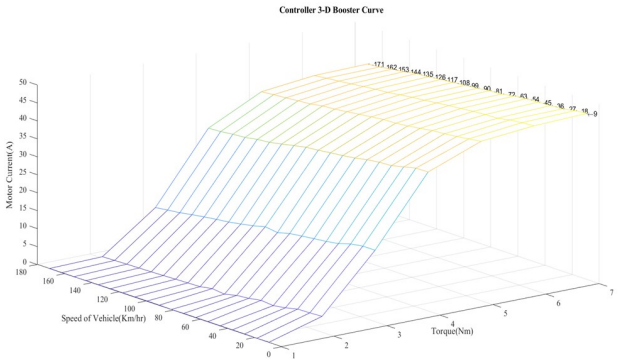

Figure 3. Characteristic boost curve

3. PIDF CONTROLLER

As widely known, the PID controller with derivative filter is employed almost in all automated industries ranging from heavy work industries to low technological industries due to its simple structure, easy implementation, good performance, cheap availability, low-price maintenance as well as less effort applicability. The transfer function of the PID controller with derivative filter is given as

$$C(s) = \frac{U(s}{R(s)} = K_p + K_i s + K_d \frac{N}{1 + N/s}. \tag{18}$$

It consists of four different parameters, namely proportional gain (K_p), integral gain (K_i), derivative gain (K_d), and the filter coefficient (N). For optimal performance, these parameters need to be tuned. Manual tuning of the PIDF controller takes time, is strenuous, and leads to poor performance. Conventional tuning methods work well for several processes, but sometimes these do not prove to be suitable tuning methods because they tune for a particular point of operation. They do not give a satisfactory response whenever there exists a variation in the operation range and produce large overshoot. If optimally tuned, the system dynamic response gets improved, the overshoot gets reduced, and the steady-state error gets eliminated, consequently improving the system stability. The basic structural block diagram is shown in Figure 4. As soon as setpoint changes, the error occurs which is computed as the differential of true output and set point. The controller actions (proportional, integral, and derivative) are generated using the error signal $E(s)$. The weighing signals emerged are summed to constitute the control action signal $U(s)$, which is then fed to the system. Again, the same process runs continuously to decrease the steady-state error.

4. APPLIED EVOLUTIONARY ALGORITHMS

A. GWO Algorithm

Inspired by the grey wolf's food hunting mechanism as well as the leadership ability [24], a new metaheuristic technique is developed called GWO algorithm. In this algorithm, wolf's pack is basically divided into a four-stage hierarchy: alpha, beta, delta and omega, which is followed sternly as shown in Figure 5. At first and superior of all, alpha is there, and the rest follow alpha. The algorithm, as shown below in Figure 6, proceeds basically by mimicking the nature of grey wolves of hunting, prey searching, encompassing the potential prey, and assault beginning on prey. The leader (alpha), which can be a male or female, makes decisions, beta wolves at the second stage help in making the decision, the delta follows beta, who are generally the elders and caretakers of the pack. Their work is to release warning if danger is there around them and have a watch on the boundaries of the territory. In the last in the hierarchy are the omega who follow all and allowed to eat in the last. Grey wolves hunt their prey in the following manner

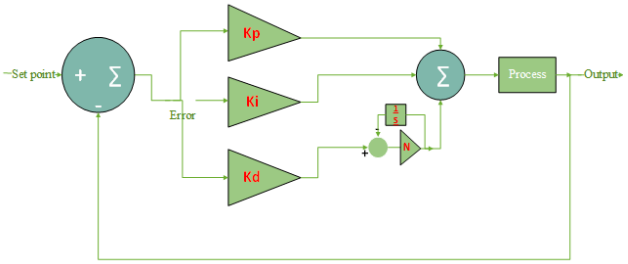

Figure 4. PID controller with derivative filter

1) Tracking and chasing their potential prey first.
2) Following, harassing, and encircling the prey.
3) Finally attacking the prey.

For the best position, encirclement proceeds as mathematically described below-

$$\vec{D} = |\vec{C}\vec{X}_p(n) - \vec{X}(n)|, \tag{19}$$

$$\vec{X}(n+1) = \vec{X}_p(n) - \vec{A}\vec{D}. \tag{20}$$

Where, n= ongoing iteration, $\vec{A}$ and $\vec{C}$ are coefficient vectors, $\vec{X}_p$ and $\vec{X}$ are position vectors, Vector A and C are found using (20) and (21)

$$\vec{A} = 2\vec{a}\vec{r} - \vec{a}, \tag{21}$$

$$\vec{C} = 2\vec{r}. \tag{22}$$

Where, $\vec{r}$ =random vector in [0,1], $\vec{a}$ =linearly decreased from 2 to 0 in each iteration, The hunting mechanism is described by the following equations,

$$\vec{D_\alpha} = |\vec{C_1}\vec{x_\alpha} - \vec{x}|, \tag{23}$$

$$\vec{D_\beta} = |\vec{C_2}\vec{x_\beta} - \vec{x}|, \tag{24}$$

$$\vec{D_\delta} = |\vec{C_3}\vec{x_\delta} - \vec{x}|. \tag{25}$$

Where, $\vec{D_\alpha}$, $\vec{D_\beta}$, $\vec{D_\delta}$ are modified new distance vectors between α, β, δ positions to other wolves and $\vec{x_1}$, $\vec{x_2}$, $\vec{x_3}$ are three coefficient vectors that help in adjusting distance vectors and are computed as under

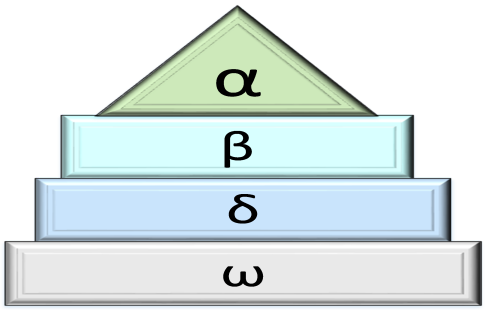

Figure 5. Social hierarchy among grey wolves

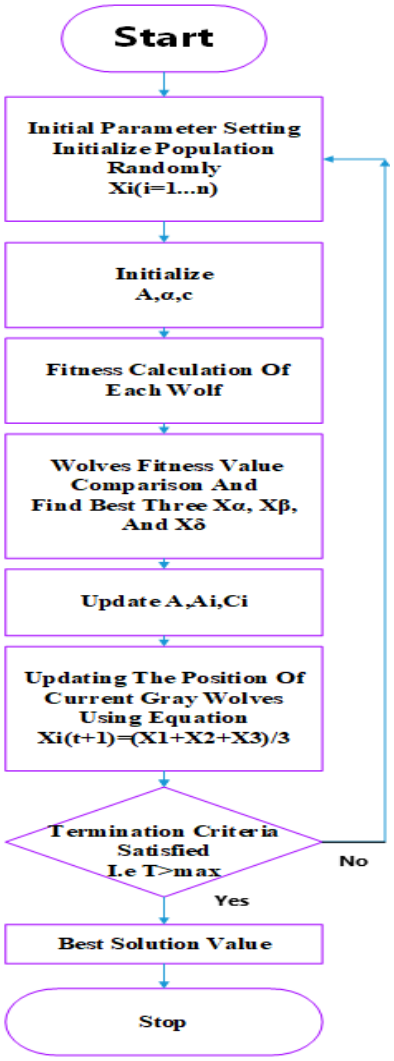

Figure 6. GWO algorithm

$$\vec{x_1} = \vec{x_\alpha} - \vec{A_1}\vec{D_\alpha}, \tag{26}$$

$$\vec{x_2} = \vec{x_\beta} - \vec{A_2}\vec{D_\beta}|, \tag{27}$$

$$\vec{x_3} = \vec{x_\delta} - \vec{A_3}\vec{D_\delta}|. \tag{28}$$

$\vec{A_1}$, $\vec{A_2}$, $\vec{A_3}$ denote coefficient vectors. The finalized position vector is computed as

$$\vec{X}(n+1) = \frac{\sum_{i=1}^{n} x_i}{3}, \tag{29}$$

Where the digit 3 in the denominator represents the number of wolves. Parameters A and C help the optimization algorithm in obtaining the optimal solution in the search space.

B. MVO Algorithm

The MVO algorithm is a nature-inspired algorithm [25]. The main inspiration of MVO is the multiverse theory, which is based on cosmology concepts involving the following three kinds of holes.

1) White hole, responsible for exploration.
2) Black hole, responsible for exploitation.
3) Worm hole, responsible for local search.

Multiverse term basically stands opposite just to universe i.e., it refers to the presence of another universe besides ours. In this theory, the universes might interact with each other and even collide sometimes as well as there may be different physical laws in each universe. In the MVO algorithm, as depicted in Figure 7, the following rules are applied for the universes.

1) Where there is a higher inflation rate, there is a low probability of a white hole presence.
2) If the inflation rate is high, that means there is a low probability of black holes presence.
3) Through white holes, the objects are favored to be sent by those universes in which there is a high inflation rate.
4) Those universes receive more objects which have a lower inflation rate.
5) Objects over the universe might go through random movement via worm holes, without putting weight on the inflation rate, towards the best universe within them.

In MVO algorithm, it is conceptualized that those universes create more white holes that have a high inflation rate and will help other universes to improve their individual's inflation rate by sending objects to them. Black hole, possibly present in universes which have low inflation rate, will receive more objects probably from others.

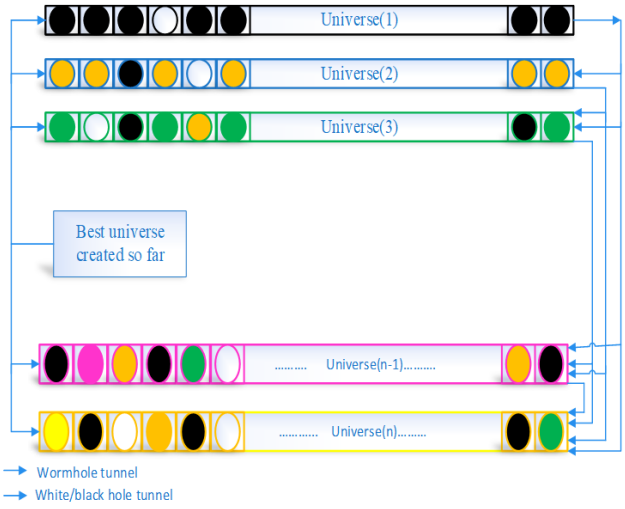

Figure 7. MVO algorithm [25]

TABLE II. CHARACTERISTIC PARAMETERS OF MANUAL, GWO AND MVO TUNED PIDF CONTROLLER

Parameter	Manual tuned PIDF controller	GWO-tuned PIDF controller	MVO-tuned PIDF controller
No. of iterations	50	50	50
No. of variables	4	4	4
No. of Agents	50	50	50
Objective function	MSE	MSE	MSE

TABLE III. CONTROLLER PARAMETER VALUES

Parameter	Manual tuned PIDF controller	GWO-tuned PIDF controller	MVO-tuned PIDF controller
K_p	250	285.1533	293.4924
K_i	10	2.7603	12.1091
K_d	2.5	0.8109	1.5561
N	75	41.7267	18.3101
MSE	$9.331e{-}08$	$8.018e{-}08$	$6.655e{-}08$

Thus, an increase in inflation rate is observed for the universe which receives objects. During this whole transportation through black hole and white hole tunnel, there is an improvement in the overall inflation rate, and the random appearance of a wormhole within universes will lead to maintaining diversity during the course. The abrupt change in universes for white and black hole tunnel helps resolve local best stagnation, and hence it assures exploration. As well as the wormhole re-span some variables about the best solution attained within all iterations randomly thus, it ensures exploitation over the most favorable region within search space.

5. SIMULATION ANALYSIS AND RESULTS

Simulation results are obtained for vehicle speed of 72 km/hr and with sinusoidal steering wheel torque in the range of $1-7Nm$. Also, the effectiveness of different tuning algorithms GWO and MVO is validated by analyzing the assist motor current supplied to the EPAS system with the objective of minimizing the current consumption of the EPAS system. The characteristic parameters of GWO and MVO algorithms are given in Table II with the optimized values of the PIDF controller parameters via these algorithms tabulated in Table III. The expected lowered assist current values obtained with PIDF- GWO and PIDF-MVO, with respect to the manually tuned PIDF controller, are presented in Table IV.

Mean squared error (MSE), as given by equation (29), is used as the main objective function for optimal tuning of the PIDF controller parameters. However, for comparative analysis, other four performance indices are also implemented as the objective functions, separately, for optimal tuning of the controller parameters. These include integral of time multiplied by absolute error (ITAE), integral of absolute magnitude of the error (IAE), integral of the squared error (ISE), and integral of time multiplied by the squared error (ITSE). Values of these performance indices, as obtained using different optimization techniques, are given in Table VII. As can be observed from Table V, the value of the MSE is the least of all with all the three tuning approaches.

$$\frac{1}{N}\sum_{1}^{N}|x(t)-\hat{x}(t)|^2. \tag{30}$$

Where, N = Data points, $x(t)$ = Actual motor current, $\hat{x}(t)$= Predicted motor current.

The results shown in Figure 8 (a to c) showcases the relative comparison of the actual assist motor current vis-à-vis the reference assist motor current in respect of different tuning approaches with PIDF controller.

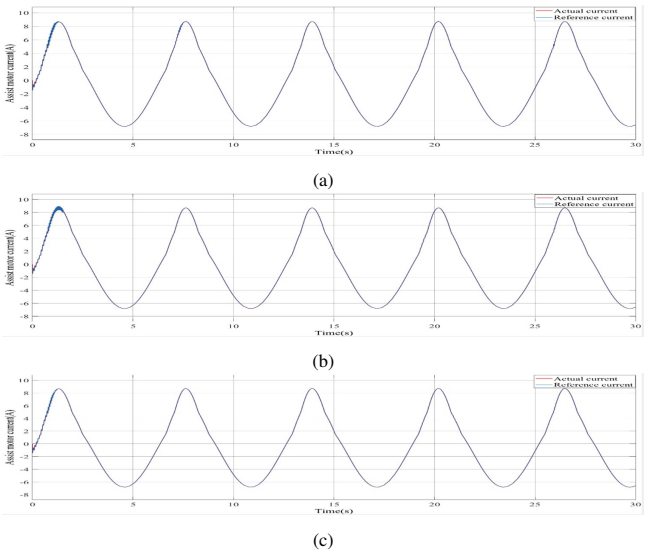

(a)

(b)

(c)

Figure 8. Assist motor current vs. Reference current (a) manually tuned PIDF controller (b) GWO tuned PIDF controller (c) MVO tuned PIDF controller

From these figures, it can be brought out that the

TABLE IV. CONTROLLER PARAMETER VALUES

Controller	Max. current value	Min. current value	Peak to Peak value	RMS value
Conventional PIDF	9.229	-6.819	16.05	5.144
GWO tuned PIDF	8.954	-6.815	15.77	4.885
MVO tuned PIDF	8.714	-6.820	15.53	4.517

TABLE V. DRIVER'S TORQUE

Tuning Algorithm	RMS value of driver's torque (Nm)
Manual tuned PIDF controller	2.580
GWO tuned PIDF controller	2.520
MVO tuned PIDF controller	2.468

TABLE VI. ASSIST MOTOR TORQUE

Tuning Algorithm	RMS value of Assist motor torque (Nm)
Manual tuned PIDF controller	$2.419e{-}01$
GWO tuned PIDF controller	$2.175e{-}01$
MVO tuned PIDF controller	$2.016e{-}01$

actual assist motor current with MVO-tuned PIDF controller almost mimics the reference assist motor current and the response is superior to that of the GWO tuned PIDF controller and the manually tuned PIDF controller in the sense that the value of the assist motor current comes out to be the least in case of MVO tuned PIDF controller.

Figure 9 shows the assist motor current with all tuning methods in a single frame for better appreciation of the results, while Figure 10 (a to c) depicts the driver's torque with the three tuning methods separately, which is also presented quantitatively in Table V. It can be observed from Figure 10 and Table V that the driver's torque is minimum with MVO-tuned PIDF controller as compared to the other two tuning methodologies. Figure 11 and Table VI showcase the assist motor torque, qualitatively and quantitatively respectively, for the three different tuning approaches with PIDF controller. The responses of the MVO tuned PIDF controller and GWO tuned PIDF controller are almost similar, however slightly better in case of MVO tuned PIDF controller. Both MVO and GWO tuned PIDF controller responses turn out to be superior to the manually tuned PIDF controller, anyway. It can be clearly seen from these results that the PIDF controller tuned using Meta-heuristic algorithms helps not only in reducing the current consumption but also increases the assist motor torque with respect to manually tuned PIDF controller.

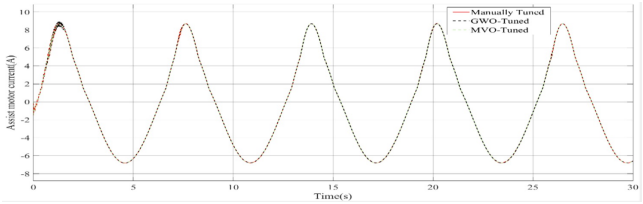

Figure 9. Assist motor current with all tuning methods in a single frame

(a)

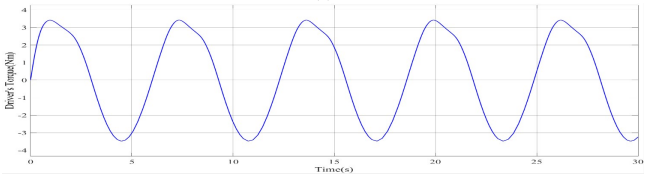

(b)

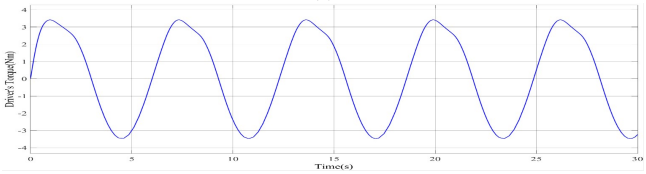

(c)

Figure 10. Driver's torque (a) manual tuned PIDF controller (b) GWO tuned PIDF controller (c) MVO tuned PIDF controller

TABLE VII. MINIMUM VALUES OF DIFFERENT PERFORMANCE INDICES

Performance Indices	Manually-tuned PIDF controller	GWO-tuned PIDF controller	MVO-tuned PIDF controller
ITAE	4.96	9.682	7.021
ITSE	0.06997	0.06797	0.8836
ISE	0.004673	0.08915	0.06517
IAE	0.3286	0.2745	1.338
MSE	$9.331e{-}08$	$8.018e{-}08$	$6.655e{-}08$

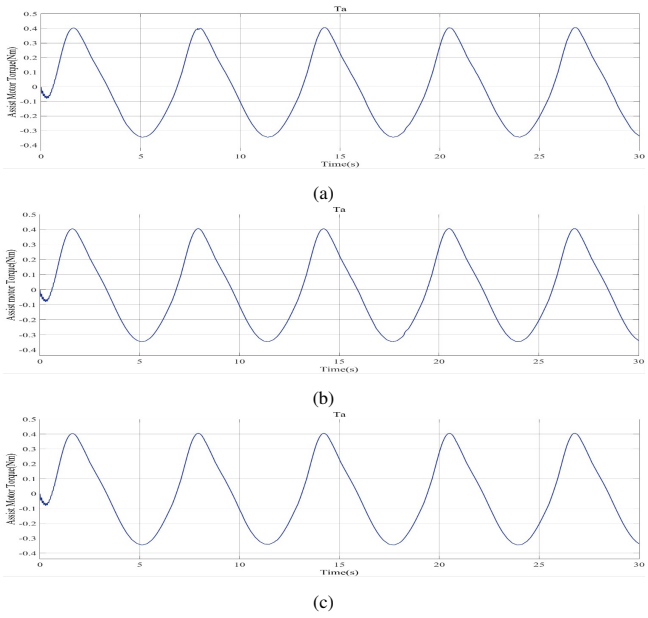

Figure 11. Assist Motor Torque (a) Manual tuned PIDF controller (b) GWO tuned PIDF controller (c) MVO tuned PIDF controller

6. CONCLUSION

The paper has explored and established the capability of various metaheuristic techniques in optimally tuning the PIDF controller parameters for the EPAS system to minimize the amount of current utilized for assist motor operation and hence reducing the burden of drawn current from EV's main storage battery. Also, the proposition has been proved effective in increasing the assist motor torque and thereby enhancing the driver's comfort. This study can be further extended to the cases with nonlinearities included, such as friction, in the mechanical system. The effect of drag on current consumption can also be investigated.

REFERENCES

[1] L. Chapman, "Transport and climate change: a review," *Journal of Transport Geography*, vol. 15, no. 5, pp. 354–367, Sep. 2007.

[2] A. A. Juan, C. A. Mendez, J. Faulin, J. De Armas, and S. E. Grasman, "Electric Vehicles in Logistics and Transportation: A Survey on Emerging Environmental, Strategic, and Operational Challenges," *Energies*, vol. 9, no. 2, p. 86, Feb. 2016. [Online]. Available: https://www.mdpi.com/1996-1073/9/2/86

[3] T. H. Hu, C. J. Yeh, S. R. Ho, T. H. Hsu, and M. C. Lin, "Design of control logic and compensation strategy for electric power steering systems," in *2008 IEEE Vehicle Power and Propulsion Conference*, Sep. 2008, pp. 1–6.

[4] A. Badawy, J. Zuraski, F. Bolourchi, and A. Chandy, "Modeling and Analysis of an Electric Power Steering System," Mar. 1999, pp. 1999–01–0399.

[5] X. Chen, X. Chen, and K. Zhou, "Optimal control of electric power-assisted steering system," in *Proceedings of 2005 IEEE Conference on Control Applications, 2005. CCA 2005.*, Aug. 2005, pp. 1403–1408.

[6] M. Parmar and J. Hung, "A sensorless optimal control system for an automotive electric power assist steering system," *IEEE Transactions on Industrial Electronics*, vol. 51, no. 2, pp. 290–298, Apr. 2004.

[7] N. Mehrabi, N. L. Azad, and J. McPhee, "Optimal disturbance rejection control design for Electric Power Steering systems," in *2011 50th IEEE Conference on Decision and Control and European Control Conference*, Dec. 2011, pp. 6584–6589.

[8] P. Shi, S. Gao, L. Miao, and H. Wang, "Optimal Controller Design for Electric Power Steering System Based on LQG," in *2009 International Conference on Information Engineering and Computer Science*, Dec. 2009, pp. 1–4.

[9] X. Li, X.-P. Zhao, and J. Chen, "Controller design for electric power steering system using T-S fuzzy model approach," *Int. J. Autom. Comput.*, vol. 6, no. 2, pp. 198–203, May 2009.

[10] C. Chitu, J. Lackner, M. Horn, P. Srikanth Pullagura, H. Waser, and M. Kohlböck, "Controller design for an electric power steering system based on LQR techniques," *COMPEL - The international journal for computation and mathematics in electrical and electronic engineering*, vol. 32, no. 3, pp. 763–775, Jan. 2013.

[11] A. Marouf, C. Sentouh, M. Djemaï, and P. Pudlo, "Control of electric power assisted steering system using sliding mode control," in *2011 14th International IEEE Conference on Intelligent Transportation Systems (ITSC)*, Oct. 2011, pp. 107–112.

[12] Z. Xue-Ping, L. Xin, C. Jie, and M. Jin-Lai, "Parametric design and application of steering characteristic curve in control for electric power steering," *Mechatronics*, vol. 19, no. 6, pp. 905–911, Sep. 2009.

[13] V. Ciarla, V. Cahouet, C. Canudas de Wit, and F. Quaine, "Genesis of booster curves in Electric Power Assistance Steering systems," in *2012 15th International IEEE Conference on Intelligent Transportation Systems*, Sep. 2012, pp. 1345–1350.

[14] H. Zhang, Y. Zhang, J. Liu, J. Ren, and Y. Gao, "Modeling and

characteristic curves of electric power steering system," in *2009 International Conference on Power Electronics and Drive Systems (PEDS)*, Nov. 2009, pp. 1390–1393.

[15] R. C. Chabaan and L. Y. Wang, "Control of electrical power assist systems: H∞ design, torque estimation and structural stability," *JSAE Review*, vol. 22, no. 4, pp. 435–444, Oct. 2001.

[16] A. Marouf, M. Djemai, C. Sentouh, and P. Pudlo, "A New Control Strategy of an Electric-Power-Assisted Steering System," *IEEE Transactions on Vehicular Technology*, vol. 61, no. 8, pp. 3574–3589, Oct. 2012.

[17] M. K. Hassan, N. A. M. Azubir, H. M. I. Nizam, S. F. Toha, and B. S. K. K. Ibrahim, "Optimal Design of Electric Power Assisted Steering System (EPAS) Using GA-PID Method," *Procedia Engineering*, vol. 41, pp. 614–621, Jan. 2012.

[18] R. A. Hanifah, S. F. Toha, S. Ahmad, and M. K. Hassan, "Swarm-Intelligence Tuned Current Reduction for Power-Assisted Steering Control in Electric Vehicles," *IEEE Transactions on Industrial Electronics*, vol. 65, no. 9, pp. 7202–7210, Sep. 2018.

[19] R. Abu Hanifah, S. F. Toha, M. K. Hassan, and S. Ahmad, "Power reduction optimization with swarm based technique in electric power assist steering system," *Energy*, vol. 102, pp. 444–452, May 2016.

[20] K. A. Danapalasingam, "Optimisation of energy in electric power–assisted steering systems," *International Journal of Electric and Hybrid Vehicles*, vol. 5, no. 2, pp. 143–154, Jan. 2013.

[21] M. K. Hassan, A. Amiri, H. Marhaban, and A. Juraiza, "Optimal Tuning of Fractional-Order PID Controller for Electric Power-Assisted Steering (EPAS) System Using Particle Swarm Optimization (PSO)," in *Control Engineering in Robotics and Industrial Automation: Malaysian Society for Automatic Control Engineers (MACE) Technical Series 2018*, ser. Studies in Systems, Decision and Control, M. Mariappan, M. R. Arshad, R. Akmeliawati, and C. S. Chong, Eds., Cham, 2022, pp. 169–182.

[22] Y. Li, G. Wu, L. Wu, and S. Chen, "Electric power steering nonlinear problem based on proportional–integral–derivative parameter self-tuning of back propagation neural network," *Proceedings of the Institution of Mechanical Engineers, Part C: Journal of Mechanical Engineering Science*, vol. 234, no. 23, pp. 4725–4736, Dec. 2020.

[23] V. Alkelin and C. Christiansen, *Alternative Input Devices for Steer-by-Wire Systems*, 2020.

[24] S. Mirjalili, S. M. Mirjalili, and A. Lewis, "Grey Wolf Optimizer," *Advances in Engineering Software*, vol. 69, pp. 46–61, Mar. 2014.

[25] S. Mirjalili, S. M. Mirjalili, and A. Hatamlou, "Multi-Verse Optimizer: a nature-inspired algorithm for global optimization," *Neural Comput & Applic*, vol. 27, no. 2, pp. 495–513, Feb. 2016.

Vinod Kumar received his M. Tech degree in control systems from National Institute of Technology Kurukshetra, Haryana, India and currently pursuing his PhD degree in the area of designing sensitivity to temperature in biomolecular circuits from the control and automation group Indian Institute of Technology Delhi, India. His research interests include systems biology, Control applications and evolutionary optimization etc.

Gunjan Chorasiya received his M. Tech degree in control systems from the National Institute of Technology Kurukshetra, India and currently pursuing his PhD degree in the area designing robustness to temperature in biomolecular circuits Indian Institute of Technology Delhi, India. His research interests include biomolecular circuit design, optimization and their applications in power systems.

Sathans Suhag received his PhD degree in the area of intelligent control and its applications to power systems from the National Institute of Technology Kurukshetra, Haryana, India, in 2012 where, he is currently serving as Professor. His research interests include intelligent control techniques, control issues in hybrid energy systems, evolutionary algorithms and their applications in power systems.